

Noise-induced degeneration in online learning

Yuzuru Sato

*RIES / Department of Mathematics, Hokkaido University, Kita 20 Nishi 10, Kita-ku,
Sapporo 001-0020, Japan*

London Mathematical Laboratory, 8 Margravine Gardens, London W68RH, UK

Daiji Tsutsui

Department of Mathematics, Osaka University, Toyonaka, Osaka 560-0043, JAPAN

Akio Fujiwara

Department of Mathematics, Osaka University, Toyonaka, Osaka 560-0043, JAPAN

Abstract

In order to elucidate the plateau phenomena caused by vanishing gradient, we herein analyse stability of stochastic gradient descent dynamics near degenerated subspaces in a multi-layer perceptron. We show that, in Fukumizu-Amari model, attracting regions exist in the degenerated subspace, and a novel type of strong plateau phenomenon emerges as a noise-induced phenomenon, which makes learning much slower than the deterministic gradient descent dynamics. The noise-induced degeneration observed herein is expected to be found in a broad class of online learning in perceptrons.

1. Machine learning as a random dynamical system

Dynamics of learning is characterised as (i) non-autonomous dynamics driven by uncertain input sequences from the external, and (ii) multi-scale dynamics which consists of slow memory dynamics and fast system dynamics. When the uncertain input sequences are modelled by stochastic processes, dynamics of learning is described by a random dynamical system. The random dynamical systems approaches, in contrast to a traditional Fokker-Planck approach in statistical physics, permits the study not only of stationary distributions and global statistics, but also of the pathwise structure of nonlinear stochastic dynamics. Quantitative properties in machine learning can be discussed with stability and bifurcation analysis.

We start with a simple model of learning given by a gradient dynamics driven by the Ornstein-Uhlenbeck process.

$$\begin{aligned} d\boldsymbol{\theta} &= -\eta \nabla_{\boldsymbol{\theta}} l(x; \boldsymbol{\theta}) dt, \\ dx &= -\gamma x dt + \kappa dW_t, \end{aligned} \tag{1}$$

where $\boldsymbol{\theta} = (w_1, \dots, w_n) \in \mathbf{R}^n$, $x \in \mathbf{R}$, $\eta, \mu, \kappa > 0$, and W_t is the Wiener process. The slope of a potential $l(x; \boldsymbol{\theta})$ with a coefficient η defines the gradient. The stationary distribution of x is given as $N(0, \sigma^2)$, where $\sigma^2 = \kappa^2/2\gamma$, when

$x(0) = 0$. The parameter γ is the decay rate of the Ornstein-Uhlenbeck process. Gradient dynamics with external force under Langevin noise has been studied in statistical and nonlinear physics (e.g. [7]). When γ is large, our model is reduced to

$$d\boldsymbol{\theta} = -\eta \nabla_{\boldsymbol{\theta}} l(x; \boldsymbol{\theta}) dt, \quad (2)$$

where x is an i.i.d. random variable subject to $\rho(x) \sim N(0, \sigma^2)$.

The *gradient descent* dynamics is given by the average dynamics of Eq. (2) with averaged potential $E_x[l(x; \boldsymbol{\theta})]$;

$$d\boldsymbol{\theta} = -\eta \nabla_{\boldsymbol{\theta}} E_x[l(x; \boldsymbol{\theta})] dt, \quad (3)$$

where $E_x[\cdot]$ denotes the ensemble average over x . In studies on machine learning, the parameter η is known as the learning rate, the external input x as the training data, and the averaged potential $E_x[l(x; \boldsymbol{\theta})]$ as the loss function that is to be minimised. The approximation in Eq. (3) corresponds to the assumption that a large set of training data x , which are i.i.d. sampled from $\rho(x)$, is given to the system at once, yielding the exact average potential $E_x[l(x; \boldsymbol{\theta})]$. For finite data set the dynamics is given as Eq. (2) and is called a *stochastic gradient descent* dynamics. The loss function $l(x; \boldsymbol{\theta})$ is typically given by a function norm $\|f(x; \boldsymbol{\theta}) - f(x; \boldsymbol{\theta}^*)\|$, where $f(x; \boldsymbol{\theta}^*)$ is the optimal function. We adopt a multi-layer *perceptron*, a class of feed-forward neural networks, as the parametric model $f(x; \boldsymbol{\theta})$. It is known that a perceptron with a single hidden layer is an universal function approximator [6].

It is also known that, in many cases, a perceptron with gradient descent learning exhibits slow relaxation to the optimal, known as a *plateau phenomenon* (see Fig. 1), which makes the dynamics of learning stagnant. The plateau phenomenon is a chain of slow dynamics near attracting regions, during which the loss function reduces extremely small amount per unit time. Each plateau or trapping is caused by a saddle set or a Milnor attractor [9] in a degenerated subspace $f(x; \boldsymbol{\theta}^d)$ in Eq. (3), resulting in slow convergence to the optimal attractors [8, 5, 18].

Learning in perceptrons with a finite batch size S , in particular with $S = 1$, is called *online learning*. Online learning is modelled by a stochastic gradient descent dynamics, which, however, is not well understood theoretically. Recently, plateau phenomena in online learning has been studied, adopting an averaged stochastic gradient descent dynamics as an approximation;

$$d\bar{\boldsymbol{\theta}} = -\eta E_x[\nabla_{\bar{\boldsymbol{\theta}}} l(x; \bar{\boldsymbol{\theta}})] dt, \quad (4)$$

where $\bar{\boldsymbol{\theta}}$ is the average of $\boldsymbol{\theta}$ at each time t [1]. However, such an approximation is not fully valid in online learning [17]. In order to elucidate the underlying mechanism of the plateau phenomena in perceptrons, we here analyse plateau phenomena in stochastic gradient descent dynamics from a viewpoint of random dynamical systems theory. We show that, in Fukumizu-Amari model, attracting regions exist in multiply degenerated subspaces, and a strong plateau phenomenon emerges as a noise-induced phenomenon.

2. Stochastic gradient descent in perceptrons

The minimal model of multi-layer perceptrons which exhibits the plateau phenomena is given as three-layer perceptrons with gradient descent dynamics

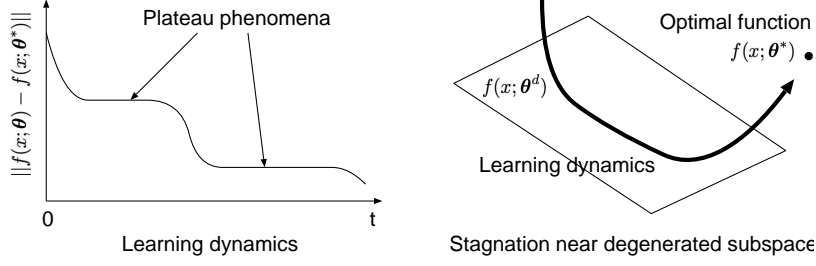


Figure 1: A schematic view of the plateau phenomena (left) and a stagnant dynamics near degenerated subspace $f(x, \theta^d)$ (right). The dynamics of learning slows down due to the vanishing gradient and eventually escapes to the optimal function $f(x; \theta^*)$.

[8].

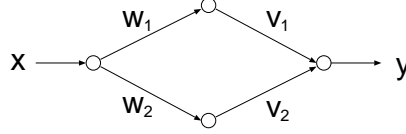


Figure 2: The three-layer perceptron: The nodes are activation functions given by $\tanh(\cdot)$, and each edge indicates a linear superposition with parameters (w_1, w_2, v_1, v_2) . The output y is a function of the input x and the parameters (w_1, w_2, v_1, v_2) .

The equation of motion of the stochastic gradient descent learning (2), can be equivalently given as the following discrete time random map;

$$\theta(t+1) = \theta(t) - \eta \nabla_{\theta} l(x; \theta(t)), \quad (t = 1, 2, \dots) \quad (5)$$

where

$$\theta = (w_1, w_2, v_1, v_2) \in \Theta \quad (6)$$

$$l(x; \theta) = \frac{1}{2} (f(x; \theta) - T(x))^2 \quad (7)$$

$$f(x; \theta) = v_1 \tanh(w_1 x) + v_2 \tanh(w_2 x). \quad (8)$$

Here, Θ is a domain of \mathbf{R}^4 called the parameter space, and x is an i.i.d. random variable subject to $\rho(x)$, $\eta \in [0, 1]$ is the learning rate, and $T(x)$ is the target function to be learnt. The Fukumizu-Amari model [8] is given by Eq. (5) with a target function

$$T(x) = 2 \tanh(x) - \tanh(4x), \quad (9)$$

and the probability distribution of the training data

$$\rho(x) = N(0, \sigma^2). \quad (10)$$

The optimal function $f(x; \theta^*)$ with parameters θ^* , which minimise $l(x; \theta)$ is given by

$$\begin{aligned} \theta^* = & (1, 4, 2, -1), (-1, 4, -2, -1), (1, -4, 2, 1), (-1, -4, -2, 1), \\ & (4, 1, -1, 2), (4, -1, -1, -2), (-4, 1, 1, 2), (-4, -1, 1, -2). \end{aligned} \quad (11)$$

The plateau phenomenon is caused by neutral stability in function space. Typically, it emerges near the degenerated subspace in the parameter space Θ . Given Eqs. (5)-(8), the following degenerated subspaces

$$\theta^d = (w, w, v_1, 2v - v_1), (w, -w, v_1, v_1 - 2v), (w_1, w, 0, 2v), (w, w_2, 2v, 0) \quad (12)$$

define a class of degenerated functions

$$f(x; \theta^d) = 2v \tanh(wx). \quad (13)$$

In this paper, we focus on interplay between degenerated subspaces $M_w = \{\theta | w_1 = w_2 = w\}$ and $M_{wv} = \{\theta | w_1 = w_2 = w, v_2 = v_1 = v\}$. In the degenerated subspace M_w , the effective degrees of freedom of Eq. (5) decreases to 3. Although we still have free variable v_1 in M_w , it does not contribute to a better function approximation. Furthermore, when a multiple degeneration to M_{wv} occurs, the effective degrees of freedom decreases to 2, and the dynamics cannot even return to the full parameter space Θ .

In many cases, the dynamics of learning stays near the degenerated subspace for a very long time. This trapping phenomenon is caused by neutral stability with vanishing gradients. Although the dynamics may eventually escape towards the global optimum by fluctuations, the dynamics of learning shows extremely slow convergence to the optimum. In some cases, the residual time near these degenerated subspace follows power-law and the system shows anomalous statistics, which is similar to intermittency in random dynamical systems [14]. In online learning, in addition to this neutrally stable trapping, “stronger” trapping based on multiple degeneration may occur as a *noise-induced phenomenon* [10, 16, 11]. We call this type of degeneration as noise-induced degeneration in online learning.

3. Strong plateau phenomena in multiply degenerated subspace

3.1. Global attraction to multiply degenerated subspace

We focus on dynamics of the following Fukumizu-Amari model;

$$w_1(t+1) = w_1(t) - \eta x v_1(t) \frac{h(x; \theta, T)}{\cosh^2(w_1(t)x)}, \quad (14)$$

$$w_2(t+1) = w_2(t) - \eta x v_2(t) \frac{h(x; \theta, T)}{\cosh^2(w_2(t)x)}, \quad (15)$$

$$v_1(t+1) = v_1(t) - \eta \tanh(w_1(t)x) h(x; \theta, T), \quad (16)$$

$$v_2(t+1) = v_2(t) - \eta \tanh(w_2(t)x) h(x; \theta, T), \quad (17)$$

where

$$h(x; \theta, T) = v_1 \tanh(w_1 x) + v_2 \tanh(w_2 x) - T(x). \quad (18)$$

The learning rate is fixed to $\eta = 0.1$. The target function is given as $T(x) = 2 \tanh(x) - \tanh(4x)$. The fluctuation σ^2 of the training data is a control parameter. Our numerical experiments suggest that, for a broad region of large σ^2 and a positive measure set of initial conditions, and for a finite time, there exists attracting dynamics from full space Θ to a degenerated subspace

$$M_w = \{\theta \mid w_1 = w_2 = w\}. \quad (19)$$

Furthermore, in some cases with large σ^2 , we observe attracting dynamics from the degenerated subspace M_w to multiply degenerated subspace

$$M_{wv} = \{\boldsymbol{\theta} \mid w_1 = w_2 = w, v_1 = v_2 = v\}. \quad (20)$$

The attraction to M_w is caused by a local minimum of the averaged potential $E_x[l(x; \boldsymbol{\theta})]$. Due to the valley formed by steep gradients of the averaged potential, the gradient dynamics is dominant compared with the stochastic effects and approaches a neighbourhood of M_w quickly (see Appendix A).

To investigate local dynamics near the degenerated subspace M_w , one can introduce the following coordinate system

$$\begin{cases} p = \frac{w_1 + w_2}{2}, & q = \frac{v_1 + v_2}{2}, \\ r = \frac{w_1 - w_2}{2}, & s = \frac{v_1 - v_2}{2}, \end{cases} \quad (21)$$

and the corresponding transformed model

$$p(t+1) - p(t) = -\frac{\eta x h}{2} \left[\frac{q(t) + s(t)}{\cosh^2((p(t) + r(t))x)} + \frac{q(t) - s(t)}{\cosh^2((p(t) - r(t))x)} \right] \quad (22)$$

$$q(t+1) - q(t) = -\frac{\eta h}{2} [\tanh((p(t) + r(t))x) + \tanh((p(t) - r(t))x)], \quad (23)$$

$$r(t+1) - r(t) = -\frac{\eta x h}{2} \left[\frac{q(t) + s(t)}{\cosh^2((p(t) + r(t))x)} - \frac{(q(t) - s(t))}{\cosh^2((p(t) - r(t))x)} \right] \quad (24)$$

$$s(t+1) - s(t) = -\frac{\eta h}{2} [\tanh((p(t) + r(t))x) - \tanh((p(t) - r(t))x)], \quad (25)$$

where

$$h(x; \boldsymbol{\theta}, T) = (q + s) \tanh((p + r)x) + (q - s) \tanh((p - r)x) - T(x). \quad (26)$$

We focus on the dynamics near M_w which approaches M_{wv} , keeping weak synchronisation near M_w . Assuming $r \simeq 0$, we have

$$s(t+1) = -\frac{\eta r x \tilde{h}}{\cosh^2(px)} + \left[1 - \frac{2\eta r^2 x^2}{\cosh^4(px)} \right] s(t) + O(r^3), \quad (27)$$

where

$$\tilde{h} = 2q \tanh((px) - T(x)). \quad (28)$$

Integration of the right-hand side of (27) over x yields

$$s(t+1) \simeq -C_1 r + [1 - C_2 r^2] s(t), \quad (29)$$

where both C_1 and C_2 are nonzero constants due to the Gaussian integral of even functions. Note that the constant C_2 is bounded. For instance, when $p > 1/4$ and $\eta = 0.1$, we have $2\eta x^2 / \cosh^4(px) < 1$ and $0 < C_2 < 1$. Assuming further that the quasi stationary density near $r = 0$ is symmetric and has the average $\langle r \rangle = 0$ and the variance $\langle r^2 \rangle \equiv \kappa < 1$, we integrate the right-hand side of (29) over the quasi stationary distribution for r , to obtain

$$s(t+1) \simeq [1 - \kappa C_2] s(t), \quad 0 < \kappa C_2 < 1 \quad (30)$$

Thus, under some conditions, the dynamics s is contracting in average and approaches 0. If s is exactly 0, we observe total synchronisation with $w_1 = w_2$ and $v_1 = v_2$ on the degenerated subspace M_{wv} . As a dynamical phenomenon, we observe (i) global attraction to a neighbourhood of M_w , and (ii) local attraction from the neighbourhood M_w to a neighbourhood of M_{wv} .

The multiple degeneration from M_w to M_{wv} is a characteristic behaviour of the stochastic gradient descent dynamics. In the case of the deterministic gradient descent dynamics, the dynamics near M_w is almost neutral in the direction of s because r converges to 0 exponentially fast. To the contrary, in the stochastic gradient descent dynamics, the dynamics of s can be contracting because r fluctuates around 0. This phenomenon is comparable with noise-induced synchronisation in random dynamical systems. A typical example of synchronisation is given by uncoupled phase oscillators driven by common noise (see Appendix D). It is known that the Lyapunov exponent of the stochastic phase oscillator is negative while those of the deterministic dynamics is zero [16, 13]. In the next section, we show that there exists yet another noise-induced trapping in the multiply degenerated subspace M_{wv} .

3.2. Attracting region in the multiply degenerated subspace

The equation of motion in M_{wv} is given by the following two-dimensional random map of $w = w_1 = w_2$ and $v = v_1 = v_2$;

$$w(t+1) = w(t) - \eta x v(t) \frac{2v(t) \tanh(w(t)x) - T(x)}{\cosh^2(w(t)x)}, \quad (31)$$

$$v(t+1) = v(t) - \eta \tanh(w(t)x) [2v(t) \tanh(w(t)x) - T(x)]. \quad (32)$$

or equivalently

$$\begin{pmatrix} w(t+1) - w(t) \\ v(t+1) - v(t) \end{pmatrix} = \eta \cdot g(x; w, v, T(x)), \quad (33)$$

where

$$g(x; w, v, T) = -[2v \tanh(wx) - T(x)] \begin{pmatrix} \frac{vx}{\cosh^2(wx)} \\ \tanh(wx) \end{pmatrix}. \quad (34)$$

The Jacobian matrix of g is given by

$$J(x; w, v) = \begin{bmatrix} -\frac{2vx^2[T(x)\tanh(wx) - 3v\tanh^2(wx) + v]}{\cosh^2(wx)} & \frac{x[T(x) - vq\tanh(wx)]}{\cosh^2(wx)} \\ \frac{x[T(x) - 4v\tanh(wx)]}{\cosh^2(wx)} & -2\tanh^2(wx) \end{bmatrix}, \quad (35)$$

or equivalently

$$\begin{aligned} J(x; w, v) &= -2 \begin{pmatrix} \frac{vx}{\cosh^2(wx)} \\ \tanh(wx) \end{pmatrix} \begin{pmatrix} \frac{vx}{\cosh^2(wx)} & \tanh(wx) \end{pmatrix} \\ &\quad - (2v \tanh(wx) - T(x)) \begin{pmatrix} -\frac{2vx^2 \tanh(wx)}{\cosh^2(wx)} & \frac{x}{\cosh^2(wx)} \\ \frac{x}{\cosh^2(wx)} & 0 \end{pmatrix} \end{aligned} \quad (36)$$

Let the eigenvalues of J at a point (w, v) be $\mu_-(x; w, v)$ and $\mu_+(x; w, v)$ ($\mu_- \leq \mu_+$) (See Appendix B). Since

$$\det \begin{pmatrix} -\frac{2vx^2 \tanh(wx)}{\cosh^2(wx)} & \frac{x}{\cosh^2(wx)} \\ \frac{x}{\cosh^2(wx)} & 0 \end{pmatrix} = -\left(\frac{x}{\cosh^2(wx)}\right)^2 < 0 \quad (37)$$

for $x \neq 0$, the second term of Eq. (36) has both positive and negative eigenvalues if $2v \tanh(wx) - T(x) \neq 0$. The first term of Eq. (36) is negative semidefinite. Thus, $\mu_-(x; w, v)$ is negative whenever $2v \tanh(wx) - T(x) \neq 0$. Therefore, for sufficiently small η , the point (w, v) is attracting when $\mu_+(x; w, v)$ is non-positive; otherwise, it is a saddle. In this way, the dynamics near (w, v) on M_{wv} is characterised by the sign of $\mu_+(x; w, v)$ as long as η is small.

We investigate the dynamics near $(w, v) = (1/2, 1/2)$ by computing the eigenvalues $\mu_{\pm}(x; 1/2, 1/2)$ of $J(x; w, v)$ explicitly. We see from (Fig.3 (left)) that the dynamics is attracted to the point $(w, v) = (1/2, 1/2)$ when the fluctuation σ^2 is sufficiently large. Put differently, the large fluctuation may “stabilise” the dynamics near (w, v) in M_{wv} . As a result, the residual time near M_{wv} is extended and a stronger plateau phenomenon is observed.

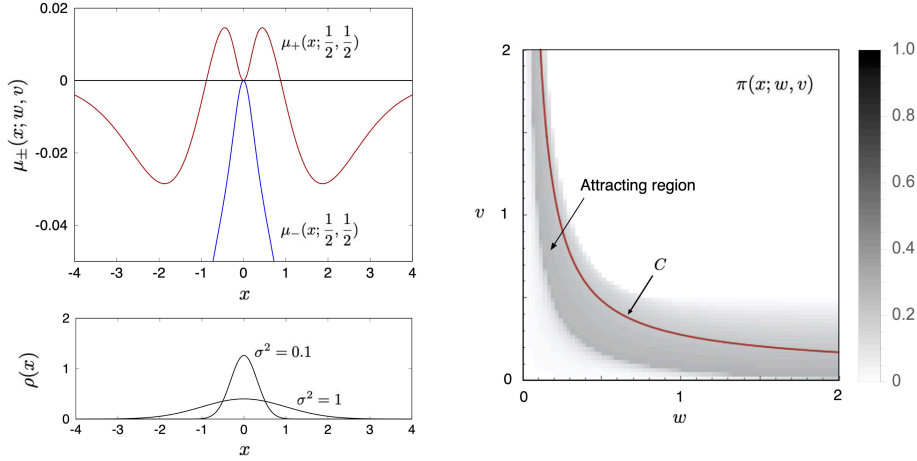


Figure 3: (Left) The eigenvalues $\mu_+(x; 1/2, 1/2)$ (red), and $\mu_-(x; 1/2, 1/2)$ (blue) of $J(x; 1/2, 1/2)$ as well as the distribution $\rho(x)$ are depicted as functions of x . The parameters are set as $T(x) = 2 \tanh(x) - \tanh(4x)$, $\eta = 0.1$, and $\sigma^2 = 0.1, 1$. When the fluctuation σ^2 is small, x is frequently sampled near zero, and the point $(w, v) = (1/2, 1/2)$ is a saddle point; otherwise, it is an attracting point. (right) The probability $\pi(x; w, v) = \text{Prob}[\mu_+(x; w, v) \leq 0]$ for $\sigma^2 = 1$ plotted in $[0, 2]^2$ on M_{wv} . The red curve C indicates the valley formed by steep gradients of the averaged potential (see Appendix A).

Fig.3 (right) shows the numerically computed probability distribution

$$\pi(x; w, v) = \text{Prob}[\mu_+(x; w, v) \leq 0], \quad (38)$$

with $\sigma^2 = 1$, where higher values of $\pi(x; w, v)$ corresponds to the darker tones. The red curve C indicates the approximated one-dimensional valley formed by steep gradients of the averaged potential. In this case, C includes a local minimum of the averaged potential. The dark grey region, where $\pi(x; w, v)$ is

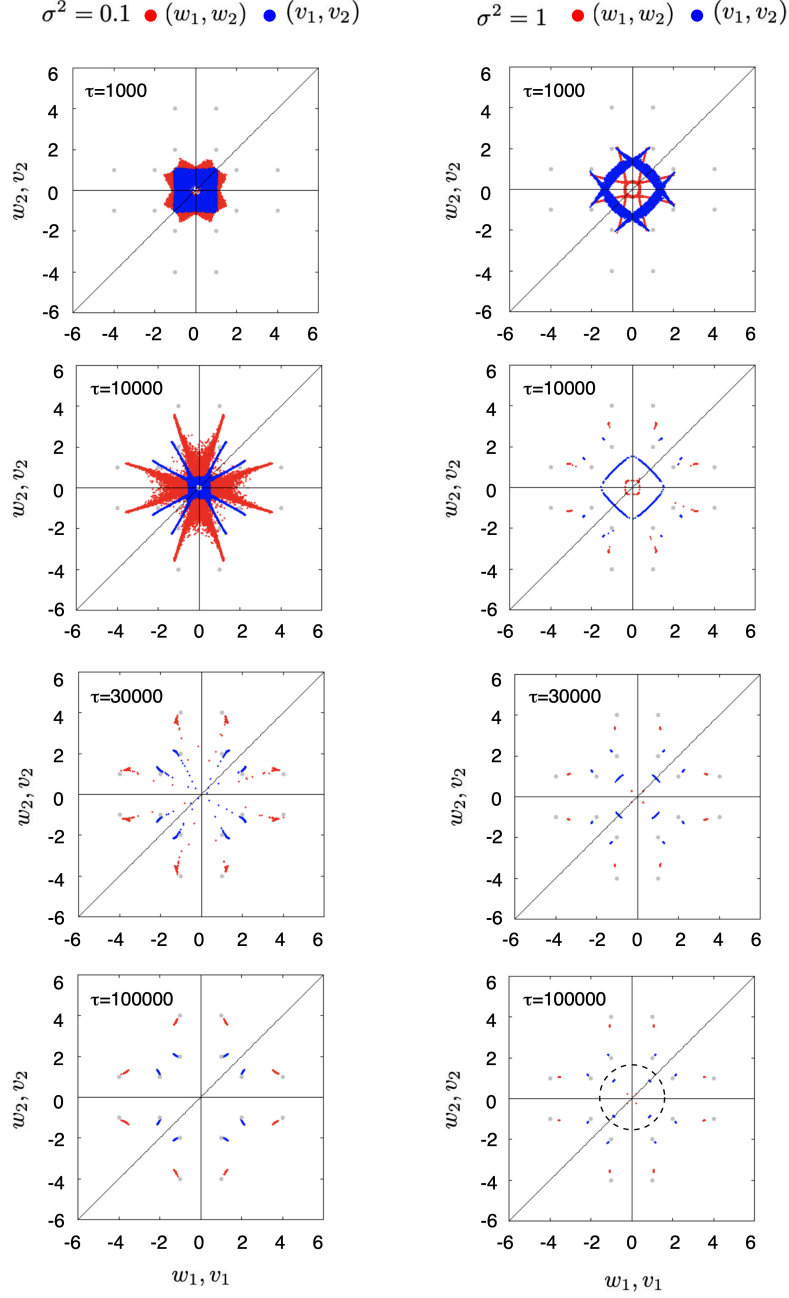


Figure 4: Finite time pullback attractors (see appendix C) with the pullback time $\tau = 1000$, $\tau = 10000$, $\tau = 30000$, and $\tau = 100000$ in the full space Θ . Parameters are set as $T(x) = 2 \tanh(x) - \tanh(4x)$, $\eta = 0.1$, and $\sigma^2 = 0.1$ (left) and $\sigma^2 = 1$ (right). The red and blue dots represent paths of (w_1, w_2) and (v_1, v_2) , respectively, starting from different initial conditions. Both dynamics are plotted together in each panel. The grey points correspond to the optimal attractors θ^* . The synchronisation manifolds $w_1 = w_2$ and $v_1 = v_2$ are depicted as a single line. A typical noise realisation $\{x\}$ is fixed and dynamics is developed with 10^5 different initial conditions $\theta(0) \in [-1, 1]^4$. When $\sigma^2 = 1$, the trapping dynamics near M_{wv} is observed in the attracting region indicated by a dashed circle.

large, may cause stronger trapping dynamics on M_{wv} . To the contrary, with smaller fluctuation $\sigma^2 = 0.1$, the grey attracting region in Fig. 3 (right) disappears because most points in M_{wv} are saddle points. Thus, there exists another noise-induced phenomenon, i.e., the emergence of an attracting region on M_{wv} due to the large fluctuation σ^2 , resulting in a substantial extension of the escape time from M_{wv} .

The global dynamics of stochastic gradient descent in Θ is shown in Fig.4. It depicts converging dynamics to pullback attractors [12] (see Appendix C) in Fukumizu-Amari model with $T(x) = 2 \tanh(x) - \tanh(4x)$, $\eta = 0.1$, and $\sigma^2 = 0.1, 1$. The red and blue dots represent paths of (w_1, w_2) and (v_1, v_2) , respectively, starting from different initial conditions. Both dynamics are plotted together in each panel. The grey points correspond to the optimal attractors θ^* . The synchronisation manifolds $w_1 = w_2$ and $v_1 = v_2$ are depicted as a single line. In the case of $\sigma^2 = 1$, clear noise-induced degeneration, i.e. $|w_1 - w_2| \rightarrow 0$ near M_w at $\tau = 10000$, followed by $|v_1 - v_2| \rightarrow 0$ near M_{wv} at $\tau = 30000$, are observed. Due to this type of noise-induced degeneration, substantial number of sample paths stay near the attracting region in M_{wv} for a extremely long time, which is shown in a dashed circle at $\tau = 100000$. In sum, noise-induced degeneration and plateau phenomena emerge through the following three process;

1. Global attraction to a neighbourhood of M_w .
2. Local attraction from the neighbourhood of M_w to a neighbourhood of M_{wv} .
3. Long term trapping near attracting regions in M_{wv} .

4. Noise induced phenomena in online learning

If there exists an attractor A on a subspace M , and A is not an attractor in the full space Θ , it is called a relative attractor in Θ [15]. Thus, if there exists an attractor on M_{wv} , it is a relative attractor. If there is no random compact invariant set in a random dynamical system, all random attractors are random Milnor attractors [2]. Our conjecture is that both relative attractors (or attracting region) in the degenerated subspaces M_{wv} and the optimal attractors in the full space Θ are random Milnor attractors. The dynamics of learning may come and go with each attractor in a long time scale.

In general, non-optimal stable random attractors may exist in stochastic gradient descent learning with small η , because $T(x)$, $f(x; \theta)$, and $\nabla_{\theta} l(x; \theta)$ are bounded for any $\rho(x)$. In these cases, if an initial point $\theta(0)$ does not belong to the effective basins of the optimal attractors, the attracting region near θ^d may become a stable random attractor and the orbits can stay there for an arbitrarily long time. Further studies on stability of attractors and bifurcations on the degenerated subspaces will be reported elsewhere.

In conclusion, in Fukumizu-Amari model, there exists characteristic fluctuation sizes of the training data, with which the dynamics shows strong plateau phenomena. Starting from an initial point in the full space, the dynamics of learning is attracted by a degenerated subspace by the gradient, and then, is attracted by a multiply degenerated subspace, which we call noise-induced degeneration. When the fluctuation size is large, in the multiply degenerated subspace, attracting region emerges. Although it is finite-time trapping and

dynamics eventually escapes to the optimal attractor, the residual time near the attracting region in the multiply degenerated subspace can be extremely long. This phenomena is expected to be observed in a broad class of online learning because of the universality of the presented noise-induced phenomena. Our approach would shed new light on various problems in machine learning from a viewpoint of random dynamical systems theory.

5. Acknowledgments

YS is supported by the external fellowship of London Mathematical Laboratory and the Grant in Aid for Scientific Research (C) No. 18K03441, JSPS. Authors are supported by the Grant in Aid for Scientific Research (B) No. 17H02861, JSPS.

Appendix A. Local minima in the averaged dynamics

In this paper, we have treated $\tanh(\cdot)$ as an activation function. However, in order to analyse the averaged potential, we herein use the function $h(u) := \operatorname{erf}(u/\sqrt{2}) := \sqrt{2/\pi} \int_0^u e^{-t^2/2} dt$ as an approximation of $\tanh(\cdot)$ to understand the qualitative behaviour of the dynamics. According to [3], for a network

$$f(x; \boldsymbol{\theta}) = v_1 h(w_1 x) + v_2 h(w_2 x), \quad (\text{A.1})$$

and a target function which is denoted as

$$T(x) = \nu_1 h(\omega_1 x) + \nu_2 h(\omega_2 x), \quad (\text{A.2})$$

for some values $\nu_1, \nu_2, \omega_1, \omega_2 \in R$, the averaged potential is given by

$$\begin{aligned} L(\boldsymbol{\theta}) &= E_x \left[\frac{1}{2} (f(x; \boldsymbol{\theta}) - T(x))^2 \right] \\ &= \frac{1}{\pi} \sum_{i,j=1}^2 v_i v_j \Phi(w_i, w_j) - \frac{2}{\pi} \sum_{i,a=1}^2 v_i \nu_a \Phi(w_i, \omega_a) + \text{const}, \end{aligned} \quad (\text{A.3})$$

$$\Phi(\zeta_1, \zeta_2) := \arcsin \left(\frac{\sigma^2 \zeta_1 \zeta_2}{\sqrt{1 + \sigma^2 \zeta_1^2} \sqrt{1 + \sigma^2 \zeta_2^2}} \right). \quad (\text{A.4})$$

When $w_1 \neq 0$ and $w_2 \neq 0$, the function $L(\boldsymbol{\theta})$ is a quadratic in (v_1, v_2) , and thus has a minimiser. In particular, when $w_1 = w_2 = w$ is fixed and $v_1 = v_2 = v$,

$$L^*(w, v) := L(\boldsymbol{\theta}) = \frac{4}{\pi} \left(v^2 \Phi(w, w) - v \sum_{a=1}^2 \nu_a \Phi(w, \omega_a) \right) + \text{const}. \quad (\text{A.5})$$

takes minimum at

$$v^*(w; \sigma^2) = \frac{\sum_a \nu_a \Phi(w, \omega_a)}{2\Phi(w, w)}. \quad (\text{A.6})$$

Hence, a minimiser of L^* lies in the one-dimensional valley $\{(w, v^*(w; \sigma^2)) | w \in R\}$.

For $(\omega_1, \omega_2, \nu_1, \nu_2) = (1, 4, 2, -1)$ and $\sigma^2 = 1$, in particular, we have the red curve C in Fig. 3 (right) as

$$v^*(w; 1) = \frac{\left(2 \arcsin \left(\frac{w}{\sqrt{2}\sqrt{1+w^2}} \right) - \arcsin \left(\frac{4w}{\sqrt{17}\sqrt{1+w^2}} \right) \right)}{\left(2 \arcsin \left(\frac{w^2}{1+w^2} \right) \right)}. \quad (\text{A.7})$$

Appendix B. Eigenvalues of Jacobian of the dynamics in the multiply degenerated subspace

The Jacobian of g on the multiply degenerated subspace M_{wv} is given by

$$J = \begin{bmatrix} -\frac{2vx^2[T(x)\tanh(wx)-3v\tanh^2(wx)+v]}{\cosh^2(wx)} & \frac{x[T(x)-vq\tanh(wx)]}{\cosh^2(wx)} \\ \frac{x[T(x)-4v\tanh(wx)]}{\cosh^2(wx)} & -2\tanh^2(wx) \end{bmatrix}. \quad (\text{B.1})$$

The eigenvalues of J are given by

$$\mu_{\pm}(x; w, v) = A \pm \frac{1}{8\cosh^4(wx)}\sqrt{B}, \quad (\text{B.2})$$

where

$$A = -1 + \frac{1 + 2v^2x^2 - vx^2\tanh(wx)T(x)}{\cosh^2(wx)} - \frac{3v^2x^2}{\cosh^4(wx)}, \quad (\text{B.3})$$

$$B = 32x^2\cosh^2(wx)C + (-1 + 16v^2x^2 - 8v^2x^2\cosh(2wx) + \cosh(4wx) + 4vx^2\sinh(2wx)T(x))^2 \quad (\text{B.4})$$

$$C = 8v^2(2 + \cosh(2wx))\sinh^2(wx) - v(6\sinh(2wx) + \sinh(4wx))T(x) + 2\cosh^2(wx)T(x)^2. \quad (\text{B.5})$$

Appendix C. Pullback attractors in random dynamical systems

Let θ acts on the probabilistic space of noise realisations Ω , and $\theta_t\omega$ is the path taken at time t by the noise realisation $\omega \in \Omega$. The random dynamical system is represented by the pair (θ, ϕ) , where ϕ denotes the dynamics in the state space X , driven by a noise realisation $\theta_t\omega$. The *pullback attractor* $A(t, \omega)$ of a random dynamical system is defined as a random invariant set of X that satisfies

$$\lim_{\tau \rightarrow \infty} \text{dist}(\phi(\tau, \theta_{t-\tau}\omega)B, A(t, \omega)) = 0, \quad (\text{C.1})$$

for any bounded set $B \subset X$, where $\text{dist}(C, D)$ denotes the Hausdorff distance between two subsets C and D of X [4].

We call the following τ -pullback image of B as *finite time pullback attractor* or τ -*pullback attractor*, which is given by

$$\tilde{A}_{\tau}^B(t, \omega) = \phi(\tau, \theta_{t-\tau}\omega)B, \quad (\text{C.2})$$

where τ is called pullback time. For a given τ , the set $\tilde{A}_{\tau}^B(t, \omega)$ represents a finite space-time structure, which may include transient orbits and densities. Each invariant sets in Fig. 4 are finite time pullback attractors with pullback time τ .

Appendix D. Noise-induced synchronisation

A stochastic phase oscillator is given by

$$d\phi = \omega dt + \sin \phi \circ dW_t, \quad (\text{D.1})$$

in Stratonovich form, where ω is a constant, $\phi \in (0, 2\pi]$ is phase on circle, and W_t is the Wiener process with $dW_t \sim N(0, \sigma^2)$. The linearisation along a fixed solution ϕ is given by

$$d\psi = \cos \phi \cdot \psi \circ dW_t, \quad (\text{D.2})$$

Let $r = \log |\psi|$, then we have

$$dr = \cos \phi \circ dW_t, \quad (\text{D.3})$$

or, equivalently in Ito form,

$$dr = -\frac{\sigma^2}{2} \sin^2 \phi dt + \cos \phi dW_t. \quad (\text{D.4})$$

Thus, the Lyapunov exponent λ of (D.1) is given by

$$\lambda = \lim_{T \rightarrow \infty} \frac{r(T)}{T} = - \lim_{T \rightarrow \infty} \frac{1}{T} \int_0^T \frac{\sigma^2}{2} \sin^2 \phi dt. \quad (\text{D.5})$$

Assuming that the fluctuation σ^2 is small, the dynamics is ergodic, and the invariant density is approximately uniform on circle, we have

$$\lambda \simeq -\frac{1}{2\pi} \int_0^{2\pi} \frac{\sigma^2}{2} \sin^2 \phi d\phi = -\frac{\sigma^2}{4} < 0. \quad (\text{D.6})$$

References

- [1] Shun-ichi Amari, Tomoko Ozeki, Ryo Karakida, Yuki Yoshida, and Masato Okada. Dynamics of learning in mlp: Natural gradient and singularity revisited. *Neural computation*, 30(1):1–33, 2018.
- [2] Peter Ashwin. Minimal attractors and bifurcations of random dynamical systems. *Proceedings of the Royal Society of London. Series A: Mathematical, Physical and Engineering Sciences*, 455(1987):2615–2634, 1999.
- [3] Michael Biehl and Holm Schwarze. Learning by online gradient descent. *Journal of Physics A*, 28:643–656, 1995.
- [4] Mickaël D Chekroun, Eric Simonnet, and Michael Ghil. Stochastic climate dynamics: Random attractors and time-dependent invariant measures. *Physica D: Nonlinear Phenomena*, 240(21):1685–1700, 2011.
- [5] Florent Cousseau, Tomoko Ozeki, and Shun-ichi Amari. Dynamics of learning in multilayer perceptrons near singularities. *IEEE Transactions on Neural Networks*, 19:1313–1328, 2008.
- [6] George Cybenko. Approximation by superpositions of a sigmoidal function. *Mathematics of control, signals and systems*, 2(4):303–314, 1989.
- [7] Davide Faranda, Yuzuru Sato, Brice Saint-Michel, Cecile Wiertel, Vincent Padilla, Bérengère Dubrulle, and François Daviaud. Stochastic chaos in a turbulent swirling flow. *Physical review letters*, 119(1):014502, 2017.

- [8] Kenji Fukumizu and Shun-ichi Amari. Local minima and plateaus in hierarchical structures of multilayer perceptrons. *Neural networks*, 13(3):317–327, 2000.
- [9] John Milnor. On the concept of attractor. In *The theory of chaotic attractors*, pages 243–264. Springer, 1985.
- [10] A S Pikovskii. Synchronization and stochastization of array of self-excited oscillators by external noise. *Radiophysics and Quantum Electronics*, 27(5):390–395, 1984.
- [11] Y Sato, TS Doan, NT The, and HT Tuan. An analytical proof for synchronization of stochastic phase oscillator. *arXiv preprint arXiv:1801.02761*, 2018.
- [12] Yuzuru Sato, Mickaël D Chekroun, and Michael Ghil. Convergence rate of snapshot attractors to random strange attractors. submitted, 2020.
- [13] Yuzuru Sato, Thai Son Doan, Jeroen SW Lamb, and Martin Rasmussen. Dynamical characterization of stochastic bifurcations in a random logistic map. *arXiv preprint arXiv:1811.03994*, 2018.
- [14] Yuzuru Sato and Rainer Klages. Anomalous diffusion in random dynamical systems. *Physical Review Letters*, 122(17):174101, 2019.
- [15] Joseph D Skufca, James A Yorke, and Bruno Eckhardt. Edge of chaos in a parallel shear flow. *Physical review letters*, 96(17):174101, 2006.
- [16] Junnosuke Teramae and Dan Tanaka. Robustness of the noise-induced phase synchronization in a general class of limit cycle oscillators. *Physical review letters*, 93(20):204103, 2004.
- [17] Daiji Tsutsui. Center manifold analysis of plateau phenomena caused by degeneration of three-layer perceptron. *Neural Computation*, 32:683–710, 2020.
- [18] Haikun Wei, Jun Zhang, Florent Cousseau, Tomoko Ozeki, and Shun-ichi Amari. Dynamics of learning near singularities in layered networks. *Neural Computation*, 20:813–843, 2008.